Conformational Analysis of Methyl−Phenyl−Siloxane Chains

Juan J. Freire,[‡] Inés F. Piérola,[†] and Arturo Horta*[,†]

Departamento de Físicoquímica (CTFQ), Facultad de Ciencias, Universidad a Distancia (UNED), 28040 Madrid, Spain, and Departamento de Química Física, Facultad de Ciencias Químicas, Universidad Complutense, 28040 Madrid, Spain

Received November 20, 1995; Revised Manuscript Received April 12, 1996[⊗]

ABSTRACT: The conformational energy of chain fragments of poly(methylphenylsiloxane) is studied, considering contributions from bond stretching, bond angle bending, bond torsion, and van der Waals interactions. Energy is minimized without constraints, so that minima correspond to fully relaxed conformations. The energy minima of this phenyl-substituted polymer differ notably from those of the parent poly(dimethylsiloxane), due to the importance of the attractive interactions between pairs of phenyl groups. For two repeat units (diad), the stable conformations occur when the pair of phenyl rings is coupled parallel, face-to-face. For three repeat units (triad), the stable conformations occur also when a pair of phenyl rings is coupled parallel, face-to-face, but not necessarily those in consecutive units. Instead, the chain can coil to couple together the phenyl rings of alternate units, leaving uncoupled the phenyl ring in between. This coiling of the chain to yield a stable conformation is a genuine triad effect that cannot be predicted from the diad energies. In longer chain sequences, the contribution of this coiled triad conformation is significant.

Introduction

Most of the useful properties of the polysiloxanes are related to their structure.[1] The atomic radius of Si is large compared to that of C, and the bonds involving Si are longer than those in hydrocarbon polymers. There is a great dissimilarity in size between the two atoms that alternate along the backbone (Si and O). Partial transfer of electronic charge occurs from the oxygen lone pairs to Si.[2] Bond angles also alternate in size along the backbone, the angle Si−O−Si being much wider than tetrahedral. The force constant for the bending of this angle is relatively low, so inversion of the angle is not difficult.[3] The torsional barriers of the Si−O bonds are comparatively low, so torsions around the backbone bonds are easy in these polymers. As a result, the Si−O backbone is very flexible from the molecular point of view.[4]

This flexibility of the Si−O backbone is common to all siloxane polymers. It confers their exceptional properties as elastomers and their very low glass transition temperatures. It is also useful for the building of lateral chain liquid crystals. The substituents add their particular contribution to the properties, depending on the nature of the lateral groups. They vary from methyl to longer alkyl groups, fluoroalkyl, phenyl, stiff fragments confering liquid crystalline properties to the material, etc. By far, the one whose molecular structure and properties have been most extensively studied is poly(dimethylsiloxane) (PDMS).[1,5]

Here, we study an asymmetrically substituted (methyl, phenyl) siloxane chain: poly(methylphenylsiloxane) (PMPS). From the structural point of view, PMPS is very interesting, because the phenyl ring introduces a chromophore in every repeat unit of the chain, and this leads to a very rich photophysical behavior.[6−16] The excimer emission from pairs of phenyl rings in PMPS is related to the equilibrium population of conformations and to the dynamics of conformational transitions in this flexible chain.[6,17−19]

Because of the relationship between molecular flexibility and properties, and also because of the relevance of conformations for photophysics, we have attempted a detailed conformational study of PMPS.

The conformational properties of PMPS have been recently reviewed.[6] Theoretical calculations of these properties have been performed by matrix multiplication methods and by Monte Carlo techniques.[20−28] In all cases, a fixed geometry for the molecule was used: fixed bond lengths and bond angles, plus rotational isomers also at fixed positions, either as discrete states[20,23,24,27] or allowing a small oscillation around these states.[21,22,25,26,28]

However, recent calculations by Mattice *et al*. on PDMS[29,30] and other poly(dialkylsiloxanes)[31,32] have shown the need for a more realistic description of siloxane chains. These authors allowed for relaxation of all the atoms, by introducing a potential energy consisting of terms for bond stretching, bond bending, torsional rotations, and interatomic van der Waals interactions. Hence, their structure is flexible in all its internal degrees of freedom and can relax. With such allowances, they found that the stable conformers of PDMS are displaced with respect to the standard positions. Also, the conformational energy is a rather smooth function of the rotational angles in the chain, with rotational states not so sharp as in typical C−C chains, and with a variety of closely spaced wide minima.[29]

When considering as substituents alkyl groups longer than methyl, there is a change in the conformational characteristics. Torsional states become better defined, with sharper minima, as the alkyl group increases in size.[31] Also, interactions between the bulky side chains enforce correlations between consecutive bonds. The chain is highly flexible due to its siloxane backbone but is constrained to perform highly coupled rotations due to the steric interactions of the bulky side groups.[32]

A similar situation might be anticipated for the chains of PMPS, since one of its substituents (phenyl) is large and planar. Hence, a conformational study with flexible molecular structure allowing for relaxation is in order with this polymer. This is the work that we describe here. But the interactions arising from the bulky phenyl rings in PMPS are not really steric. As first deduced by Mark and Ko,[20] contrary to what happens

[†] Universidad a Distancia.
[‡] Universidad Complutense.
[⊗] Abstract published in *Advance ACS Abstracts,* June 1, 1996.

S0024-9297(95)01735-9 CCC: $12.00

in the vinyl chains, where steric repulsions due to atom crowding are the dominant interactions between side groups, in the case of PMPS, the interactions between pendant groups are attractive, particularly when two phenyl rings are involved, due to the relatively large intergroup separations dictated by the long Si−O bond and the wide Si−O−Si angle that build the siloxane backbone.

The conformation in which two phenyl rings are in front of each other, in a parallel orientation (sandwich-like), is a preformed dimer for excimer emission, or an excimer-forming site (EFS). Due to the attractive nature of the phenyl−phenyl interaction in PMPS, the EFSs are the most stable states.[17,18] This, together with the greater conformational flexibility of the siloxane chain, as compared to the carbon chains of vinyl polymers, may help in understanding the distinct photophysical behavior observed with PMPS.[19]

In our work of mapping the conformations of PMPS, we have to consider the different tactic forms of the polymer, a complication not present in PDMS or the other symmetrically substituted poly(dialkylsiloxanes) studied up to now with relaxed structures. Also, an oligomer related to PMPS, pentamethyltriphenyltrisiloxane, has already been analyzed with relaxation.[2]

Methods

The Si atoms are substituted asymmetrically in the PMPS chain. Hence, the diads can have two steric forms, meso (m) and racemic (r), and the triads can have three steric forms: iso (mm), syndio (rr), and hetero (mr or rm). All these are considered in our conformational analysis.

In the process of building these structures, we define the stereochemistry taking as reference for each Si atom the plane defined by the bonds O−Si−O flanking it (with the bond angle drawn open up, as a "V"). For a pair of consecutive silicons, we arbitrarily choose the m configuration, with both phenyl rings in front of their respective planes, and the r configuration, with the first (leftmost) phenyl ring in front and the second phenyl ring behind their respective planes. When the r configuration follows another r configuration, as in an rr triad, then this second r is inverted, obviously. In this way, our m and r structures are *dd* and *dl* (*ld*, if r follows another r), respectively, in the convention adopted by Mark and Ko.[20]

The computer software used is Biosym,[33] with adequate modifications of the CVFF force field. As energy components we consider bond stretching, bond angle bending, torsion around bonds, and nonbonded van der Waals interactions, without cross terms. The structural and interaction parameters used in the modified force field are as follows.

Mattice *et al.*[29] chose the energetic parameters for alkylsiloxanes to make them compatible with the results determined from *ab initio* quantum computations and the more recent conventional molecular mechanics considerations. The same energy and geometry parameters selected by Mattice *et al.*[29] are used here for the siloxane backbone and the methyl groups. Additional parameters are required in PMPS to represent the aromatic carbons. They are chosen equal to those of aliphatic carbons in the stretching of Si−C and C−H bonds, the bending of O−Si−C and C−Si−C valence angles, and the torsion of X−Si−C−X dihedral angles. For nonbonded interactions, a comparison between the van der Waals parameters, R_0 (distance) and e_0 (energy), obtained from Mark and Ko[20] and those of Mattice *et al.*[29] was the starting point. For the aliphatic carbons, both sets give the same value of R_0 and different values of e_0. For aromatic carbons, the value of R_0 obtained from Mark and Ko is accepted, and their value of e_0 is modified in the same proportion needed to bring their value of aliphatic carbons into coincidence with that of Mattice *et al.*

Energy minimization is performed by running module Discover,[33] with algorithm VA09A, until the root-mean-squared energy gradient is below 0.001 kcal mol^{-1} Å^{-1}. Molecular dynamics trajectories are also run with module Discover,[33] at a temperature of 300 K, which is maintained by instantaneous rescaling of velocities whenever the current temperature differs from the target by more than 10 K.

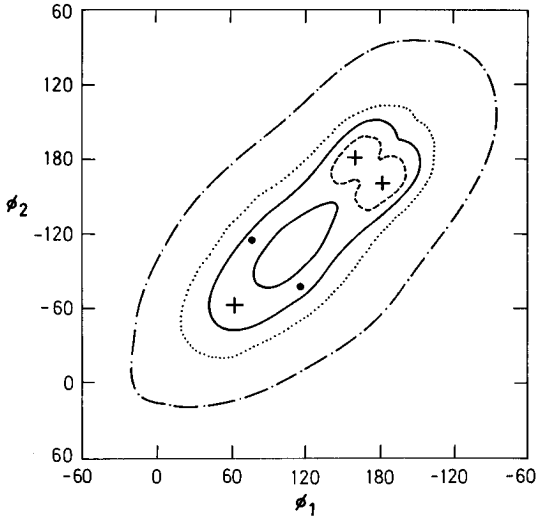

Figure 1. Map of conformational energy for an isolated meso diad of PMPS. +, Minima; ●, saddle points. Contour lines: - - -, 0.2 kcal; —, 0.5 kcal; ···, 1.0 kcal; —·—, 2.5 kcal.

Chart 1. Diads and Triads

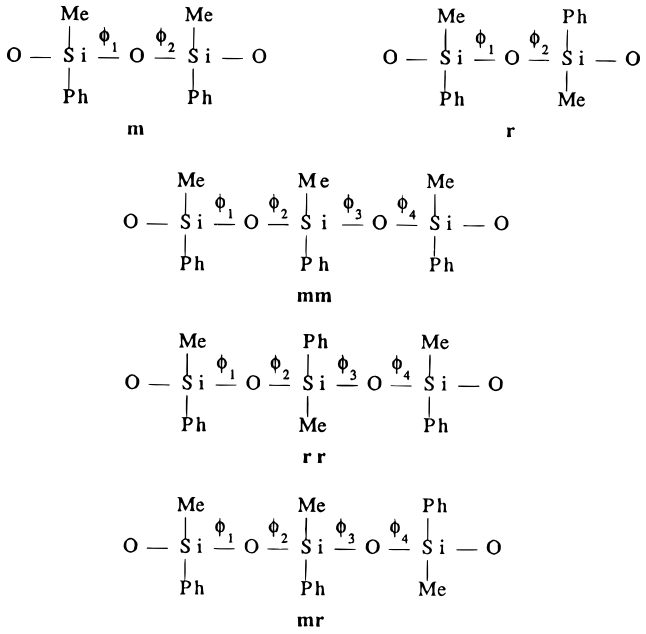

Results and Discussion

Diads. The meso and racemic diads studied are shown in Chart 1. Rotational angles ϕ_1 and ϕ_2 were scanned at 5° intervals. For each pair of values ϕ_1,ϕ_2, the energy is minimized with relaxation of all degrees of freedom, except ϕ_1,ϕ_2, which are constrained to their fixed values. Once the grid of energy versus ϕ_1,ϕ_2 is constructed in this way, the exact locations of the minima are determined by allowing for full relaxation from a nearby grid point. The resulting energy maps are shown in Figures 1 and 2, and the exact locations of minima and saddle points are given in Table 1.

We can see that the minima occur close to the rotational isomers, *t*, g^+, and g^-, but are not exactly in their nominal values of 180°, 60°, and −60°. The displacement of minima from these nominal values can reach up to about ±20° (Table 1). We can see also that

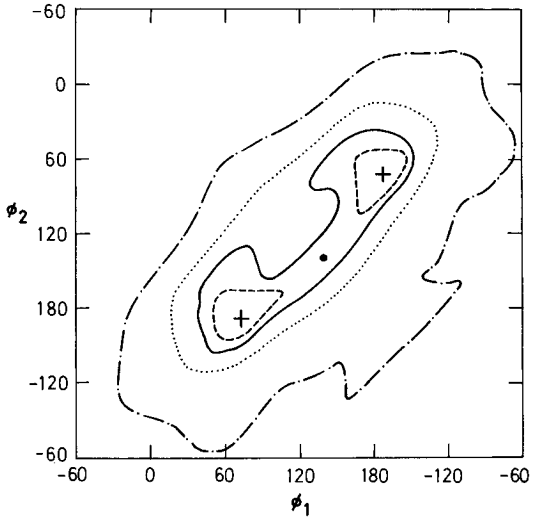

Figure 2. Map of conformational energy for an isolated racemic diad of PMPS. +, Minima; ●, saddle points. Contour lines: - - -, 0.2 kcal; —, 0.4 kcal; ···, 1.0 kcal; —·—, 2.5 kcal.

Table 1. Rotational States, Energy, and Separation between Phenyl Rings at the Minima and Saddle Points of the Diad Energy Maps of Figures 1 and 2

diad	ϕ_1 (deg)	ϕ_2 (deg)	energy[a] (kcal)	state	Ph−Ph[b] (Å)
m	161.3	178.3	0.00	minimum *tt*	3.59
	−178.3	−161.3	0.00	minimum *tt*	3.59
	63.3	−63.3	0.40	minimum g^+g^-	3.56
	116.9	−78.7	0.41	saddle	3.68
	78.7	−116.9	0.41	saddle	3.68
r	−172.2	72.1	0.00	minimum tg^+	3.56
	72.1	−172.2	0.00	minimum g^+t	3.56
	139.3	139.3	0.21	saddle	3.70

[a] Relative to the absolute minimum of the diad. [b] Between centers of mass of phenyl rings.

the *tt* state of the m diad appears to be split into two closely spaced minima (Figure 1). These features are common with PDMS,[29] where the minima are also displaced from the standard rotational isomer values and the two-bond rotational states are split into multiple minima.

We can see that the energy surface of the PMPS diads has a very profound localized well. At the bottom of the well are the different minima and saddle points. Differences in energy at this bottom (between minima and saddles) are small, below 0.5 kcal. However, the walls enclosing the well are high, about 3 kcal. Thus, within the well there are almost no energy barriers for the transition from one minimum to another. More than localized states, we have corridors of states with almost constant energy. The big energy barrier appears only when jumping out of the well.

The form of the corridor is different depending on tacticity. In the racemic diad there are two absolute minima, corresponding to the tg^+ and g^+t states. The corridor extends between these two states through the saddle, which is only 0.21 kcal above the minima. In the meso diad, the absolute minimum is split, corresponding to the *tt* state. There is another minimum corresponding to the g^+g^- state, which is 0.40 kcal above. The corridor embraces these two *tt* minima and extends to the g^+g^- state through two saddles of only 0.41 kcal.

The rotational angles change along each corridor, but the energy is kept with little variation. The passage from one minimum state to another is a transition that involves a two-bond rotation (for example, $tg^+ \leftrightarrow g^+t$, in the racemic diad). The corridor offers a path for such transitions in which the energy is kept almost without variation (maximum energy change in the example, 0.21 kcal). Each pair of backbone bonds can rotate almost isoenergetically along the corridor.

Table 2. Influence of Electrostatic Nonbonding Interactions on the Minima and Saddle Points of the Diad Energy Maps of Figures 1 and 2

diad	ϵ[a]	ϕ_1 (deg)	ϕ_2 (deg)	E^b (kcal)	ϕ_1 (deg)	ϕ_2 (deg)	E^b (kcal)	ϕ_1 (deg)	ϕ_2 (deg)	E^b (kcal)
m	∞	161	178	0.00	63	−63	0.40	117	−79	0.41
	5	156	−179	0.00	66	−66	0.31	116	−76	0.26
	3	152	−177	0.00	68	−68	0.25	117	−75	0.15
	2	145	−174	0.00	70	−70	0.19	118	−74	0.03
	1.7	141	−171	0.03	71	−71	0.21	119	−73	0.00
	1.5	137	−169	0.08	120	−73	0.00	120	−73	0.00
	1	73	−127	0.00	127	−73	0.00	127	−73	0.00
r	∞	−172	72	0.00	139	139	0.21			
	5	−171	76	0.00	142	142	0.23	101	101	0.37
	3	−171	78	0.00	144	144	0.23	102	102	0.30
	2	−171	82	0.00	146	146	0.22	102	102	0.22
	1.7	−170	84	0.00	147	147	0.21	102	102	0.09
	1.5	−170	86	0.00	149	149	0.19	103	103	0.12
	1	−170	92	0.09	154	154	0.21	104	104	0.00

[a] Dielectric constant. [b] Energy, relative to the absolute minimum of the diad, for the given value of ϵ.

Not only the energy but also the distance separating the two phenyl rings is kept practically constant along the corridor. The minima of the diad are all EFSs; that is, the two phenyl rings adopt a parallel sandwich-like conformation. But they are also EFSs at the saddles and all along the corridors (see the separation between phenyl rings in Table 1). The transitions between energy minima within the well occur thus without breaking the EFS conformation. The pairs of backbone rotational angles change along the corridor, but the phenyl rings are kept always in a parallel sandwich-like conformation. This is possible thanks to the adaptability of the relaxing structure now considered.

The reason for this constancy lies in the importance of the attraction between phenyl rings. This is the dominant interaction in these structures. The backbone of siloxane is flexible enough to follow what the nonbonded interactions (mainly those between phenyl rings) demand.

The energy surface is concave upward only for states that are EFSs (Figures 1 and 2). The conclusion is that only EFS states are stable in a diad of PMPS.

Electrostatic Nonbonding Interactions. Electrostatic nonbonding interactions are known to be of importance for the conformation of siloxane molecules.[34] The relative importance of these interactions should be less in PMPS than in PDMS, however, because of the dominant effect played by the attraction between Ph rings. This attraction, together with the torsional flexibility of the siloxane backbone, is the main responsible for the results we have just described for the diads. But the question is, how much could these results be modified by the introduction of electrostatic nonbonding interactions? To get an answer, we repeat the calculations adding now the Coulombic term between partial charges in the CVFF force field. This is done at several values of the dielectric constant, ϵ, from $\epsilon = \infty$ (no electrostatic interactions) to $\epsilon = 1$ (vacuum). The results are shown in Table 2. It contains the stable states reached in the process of minimization (this includes the saddles, because they are also tiny minima). Only one state is shown when two symmetrical, identical minima occur. Thus, the states (−161°,−178°) and

(79°,−117°) (not shown) behave equal to the states (161°,178°) and (117°,−79°), respectively, in the m diad, and the state (72°,−172°) (not shown) behaves equal to the state (−172°,72°) in the r diad.

The results in Table 2 start with no electrostatic interactions ($\epsilon = \infty$, the same results of Table 1) and gradually increase the strength of such interactions by decreasing ϵ. The value of ϵ can be fitted to reproduce the dipole moment of a representative molecule. For disiloxane, the dipole moment calculated with the parameters of the force field reproduces the experimental value ($\mu = 0.38$ D) when $\epsilon = 1.7$.

To see the influence of electrostatic nonbonding interactions, we compare the results for this $\epsilon = 1.7$ with those of $\epsilon = \infty$. First we consider the r diad. The two absolute minima continue to be such absolute minima, but slightly displaced, and the saddle at 0.21 kcal continues at this same energy. A new saddle appears with energy 0.09 kcal, but if we look at Figure 2, it is located symmetric to the previous one, so that the form of the energy well is kept entirely similar, only of more regular shape. Now the m diad. The two saddles and the two absolute minima become of practically equal energy (difference 0.03 kcal), and the g^+g^- minimum changes from 0.40 to 0.21 kcal.

As we see, the introduction of electrostatic nonbonding interactions maintains the same gross features described already: (i) there is a very profound localized well, at the bottom of which are the minima and saddle points, and (ii) within this well, there are corridors of states with almost constant energy. In fact, all the energy values of Table 2 are below 0.5 kcal, regardless of the value of ϵ. What changes is the fine detail, i.e., the exact locations of the minima and saddles (but with small displacements, at most 20°) and the very small differences in their relative stability.

Terminal Pseudoatoms. The structures studied are not real molecules because they have no terminal pseudoatoms (Chart 1). It is common practice to terminate structures with CH_3 groups. In the case of siloxane diads and triads, this is not advisable, because the C−O bond is too short (1.20 Å) and introduces severe steric constraints, not present in the Si−O backbone, which affect the nearby units. If the structures were long and the terminal CH_3 groups far from the Si−O bonds whose conformations were being considered, this would be allowed, but here it would be an unacceptable distortion. There is no software problem in studying the structures of Chart 1. However, we have to be sure that the results are not artificial. To check this point, we repeat the calculations, end-capping the structures of Chart 1 so as to convert them into real molecules. As terminal pseudoatoms, we use (i) just the H atom and (ii) the SiH_3 group, which is equivalent of the commonly used CH_3, but with the longer bond length proper of the siloxane backbone. Both ends are capped with the same group in each case.

The minimization process of these molecules is started with the terminal bonds in trans, but no constraint is imposed, so that the final structure is relaxed in all bonds. The results are shown in Table 3, just for the r diad. As we can see comparing these results with those of Table 1, the effect of introducing terminal pseudoatoms, be it H or SiH_3, is minimal, so that a more detailed report of the other structures is not needed.

Triads. A triad can be viewed as a pair of consecutive diads sharing the central atom. Four rotational bonds are in the triad, two in the first diad and two in the second diad (Chart 1). Taking into consideration just the results described above for a diad, one could expect that the only stable conformations for a triad should be those in which at least one of the two diads forms an EFS.

Table 3. Minima and Saddle Points for the r Diad End-Capped with Terminal R Pseudoatoms: R−O−Si(MePh)−O−Si(MePh)−O−R

R	ϕ_1 (deg)	ϕ_2 (deg)	E^a (kcal)
H	−173.4	73.8	0.00
	73.8	−173.4	0.00
	139.3	139.3	0.20
SiH_3	−174.2	70.2	0.00
	70.2	−174.2	0.00
	137.8	137.8	0.29

[a] Energy, relative to the absolute minimum of the molecule.

Table 4. Rotational States and Energy at Low Minima of the Triads

triad	ϕ_1 (deg)	ϕ_2 (deg)	ϕ_3 (deg)	ϕ_4 (deg)	E^a (kcal)	state	EFS[b]
iso (**mm**)	160.3	−179.6	179.6	−160.3	0.00	*tttt*	1−2−3
	177.7	−69.8	−66.8	−61.9	0.17	$tg^-g^-g^-$	1−3
	61.9	66.8	69.8	−177.7	0.17	$g^+g^+g^+t$	1−3
	−179.5	−164.7	50.9	−142.6	0.42	ttg^+t	1−2
	142.6	−50.9	164.7	179.5	0.42	tg^-tt	2−3
	176.7	−166.8	37.4	−118.8	0.42		1−2
	118.8	−37.4	166.8	−176.7	0.42		2−3
syndio (**rr**)	73.5	−173.9	173.9	−73.5	0.00	g^+ttg^-	1−2−3
	53.4	167.6	−63.1	−85.4	0.08	$g^+tg^-g^-$	1−2
	85.4	63.1	−167.6	−53.4	0.08	$g^+g^+tg^-$	2−3
	−177.2	66.1	−179.5	−74.9	0.09	tg^+tg^-	1−2−3
	74.9	179.5	−66.1	177.2	0.09	g^+tg^-t	1−2−3
	174.7	−65.3	−69.8	−61.7	0.32	$tg^-g^-g^-$	1−3
	61.7	69.8	65.3	−174.7	0.32	$g^+g^+g^+t$	1−3
	60.9	49.0	−92.9	−65.0	0.48		1−3
	65.0	92.9	−49.0	−60.9	0.48		1−3
hetero (**mr**)	161.0	179.1	−174.8	73.4	0.00	$tttg^+$	1−2−3
	177.4	−65.9	−65.3	173.6	0.12	tg^-g^-t	1−3
	176.9	−163.2	−12.1	−179.1	0.14		1−2
	161.6	−178.9	147.7	128.0	0.15		1−2−3
	167.6	179.2	71.4	179.6	0.17	ttg^+t	1−2−3
	179.7	−163.4	58.0	90.4	0.18		1−2
	147.6	−56.9	169.6	52.7	0.32	tg^-tg^+	2−3
	59.7	68.5	73.9	59.3	0.41	$g^+g^+g^+g^+$	1−3
	152.6	−16.7	139.2	66.0	0.45		2−3
	−113.1	178.6	45.9	162.7	0.46		2−3
	155.0	−62.5	−62.7	−88.2	0.47		1−3

[a] Energy, relative to the absolute minimum of the triad. [b] Phenyl rings forming EFSs.

We search for stable states of the triad by scanning the angles ϕ_1, ϕ_2, ϕ_3, and ϕ_4 at 60° intervals and minimizing the energy from these starting conformations. The results are shown in Table 4 for the lower energy states of the isotactic (mm), syndiotactic (rr), and heterotactic (mr) triads.

Several points are noteworthy. The displacement of the minima from the nominal 180°, 60°, and −60° positions is now larger than in the case of the diads. In the triad, it reaches up to about ±60°, making the assignment of conformational states to the *t*, g^+, and g^- rotational isomers meaningless in some cases. Besides, many minima occur in a very short range of energies, so the distribution of states is almost continuous.

The final stable conformations for the triad are all of the EFS type. They include the ones expected, in which at least one of the diads is in an EFS state, but they include others as well. If we number the three monomer units of the triad as 1, 2, and 3, the diad EFSs can be of the type 1−2 (formed between phenyl rings of units 1 and 2), 2−3 (formed between phenyl rings of units 2 and

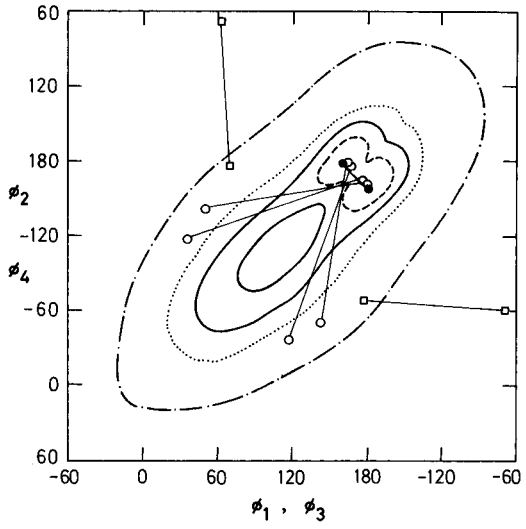

Figure 3. Low-energy conformations (E < 0.5 kcal) for an isolated isotactic triad of PMPS, plotted over the meso diad energy map. Each triad conformation is represented by a pair of points connected through a straight line. One point in the pair gives ϕ_1,ϕ_2, and the other gives ϕ_3,ϕ_4. ●—●, 0.00 kcal; □—□, 0.17 kcal; ○—○, 0.42 kcal.

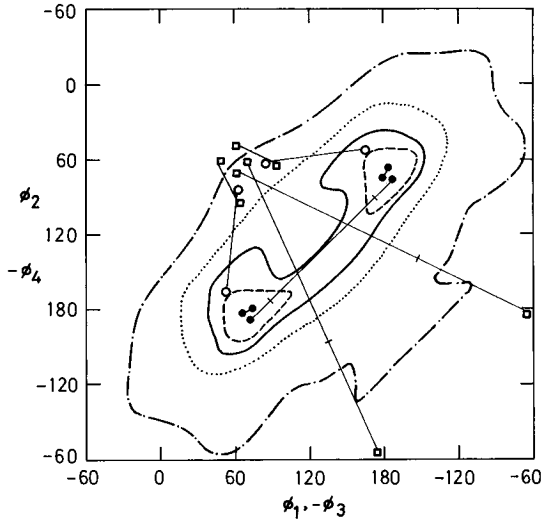

Figure 4. Same as in Figure 3, for an isolated syndiotactic triad, plotted over the racemic diad energy map. ●—|—●, 0.00 kcal; ○—○, 0.08 kcal; ●—●, 0.09 kcal; □—|—□, 0.32 kcal; □—□, 0.48 kcal.

3), or even 1−2−3 (if all three phenyl rings of units 1, 2, and 3 stack together in a three-layered sandwich).

But the triads produce also another type of EFS (Table 4), which cannot be described in terms of diad EFSs. It is the type 1−3, in which the phenyl rings that stack together forming an EFS are the ones of the end units 1 and 3, while that of the intermediate unit 2 stays apart. The phenyl rings 1 and 3 are placed parallel, facing each other, at a distance (centers of mass) of 3.7 Å, similar to that of the typical EFS between nearest neighbors (3.6 Å, Table 1). This 1−3 type of triad EFS is of energy comparable to the ones of the other types (Table 4) and is thus of similar importance in considering the average properties of the polymer.

We can visualize these different types of stable states of the triad by plotting them over the diad energy map. This is done in Figure 3 for the isotactic triad (mm, plotted over the map of the meso diad) and in Figure 4 for the syndiotactic triad (rr, plotted over the map of the racemic diad). In these figures, each triad is represented by two points, one corresponding to its first diad (ϕ_1,ϕ_2), and the other corresponding to its second diad (ϕ_3,ϕ_4), and both points are connected by a straight line.

We see that the lower energy states are achieved in the triad by widely different combinations of diad states. Some use the stable diad states close to the diad minima. But others use states which in the diad are of high energy (2−3 kcal), lying even outside the diad well. Notably, the triad states with EFSs of type 1−3 place both diads in these high-energy regions. Nevertheless, the resulting conformation for the triad is of low energy. The reason is the dominant role played by the attractive interactions between phenyl rings, which in the triad includes the possibility of 1−3. The question now is, how important are these 1−3 EFS conformations relative to the other EFS conformations of the triad? We attempt to give an approximate answer by running molecular dynamics trajectories. In these trajectories, we analyze the distances between phenyl rings (center of mass) and count the time during which such distances fall below a certain maximum value. Choosing 4.0 Å for this cutoff distance, the answer to the question posed above is that, of all EFSs formed in the triad, about 30% are of type 1−3.

This is a significant figure. The importance of these 1−3 conformations should be even larger in long chains than in the isolated triad, because in the triad there are two possibilities of forming EFSs between nearest neighbors (1−2 and 2−3) and only one possibility for the type 1−3, while in the long chain the numbers of both possibilities are practically equal. Thus, the contribution from these 1−3 conformations is high enough not to be neglected. However, in the standard treatment of polymer conformational properties, only interactions between two consecutive units are taken into account. The deficiency can, in this case, be of importance.

Another question arises. If the interactions of type 1−3 are important in the triad, could longer range interactions (1−4, 1−5, etc.) be significant in chain fragments with more units (tetrads, pentads, etc.)? The attraction between phenyl rings is dominant and may give some weight to such longer range effects. Again we attempt to obtain an approximate answer by running molecular dynamics trajectories, this time with a chain fragment of 11 monomer units. We choose just one tacticity, the perfect heterotactic chain (...mrmr...). Real polymers are not stereoregular, but their most abundant triads are heterotactic.[24] The analysis of the trajectories shows that only the EFSs of types 1−2 and 1−3 are of prime importance. Those of type 1−4 occur, but 1 order of magnitude less frequently, and those of type 1−5 are practically negligible.

The triad results can serve also to analyze the relative stability of EFSs in meso and racemic diads. By looking at the heterotactic triad (Table 4), we see that the EFSs in the meso diad are of slightly lower energy than those in the racemic diad. This relative stability holds true also in the chain, as is shown by the molecular dynamics trajectories of the longer fragment described above, where the EFSs in meso diads appear slightly more frequently than those in racemic diads.

Another effect detected by considering triads is the relative stability of the minima in meso diads. The meso diad has a split minimum around *tt* and another minimum close to g^+g^- (Figure 1). But, in the isotactic triad, neither of its two meso diads populates this g^+g^-

minimum in the lower energy states (Figure 3). The first triad state containing a g^+g^- diad appears at 1.57 kcal. The reason is that the g^+g^- conformation is a coiled one, which is restricted by the addition of another unit in the triad. This is more likely to happen inside a long chain. This is confirmed by the molecular dynamics trajectories of the longer chain fragment, where the g^+g^- state appears less frequently than any other diad state.

Acknowledgment. This work has been supported by DGICYT (Spanish Ministerio de Educación y Ciencia), under Grants PB92/0227 and MAT93-0167, and by UNED. In the early stages of the work, we benefited from the computation resources of the Aula de Diseño Molecular, Facultad de Ciencias Químicas, Universidad Complutense.

References and Notes

(1) *Silicon Based Polymer Science*; Zeigler, J. M., Fearon, F. W. G., Eds.; Advances in Chemistry Series 224; American Chemical Society: Washington, DC, 1990.
(2) Grigoras, S., Lane, T. H. In Ref 1.
(3) Debolt, L. C.; Mark, J. E. *J. Polym. Sci.: Polym. Phys. Ed.* **1988**, *26*, 989.
(4) Mark, J. E. In ref 1.
(5) Semlyen, J. A., Clarson, S., Eds. *Siloxane Polymers*; Prentice Hall: Englewood Cliffs, NJ, 1993.
(6) Horta, A.; Piérola, I. F.; Maçanita, A. L. In *Polymeric Materials Encyclopedia*; Salamone, J. C., Ed.; Chemical Rubber Co. Press: Boca Raton, FL, 1996.
(7) Salom, C.; Horta, A.; Hernández-Fuentes, I.; Piérola, I. F. *Macromolecules* **1987**, *20*, 696.
(8) Salom, C.; Gómez-Antón, M. R.; Horta, A.; Hernández-Fuentes, I.; Piérola, I. F. *Macromolecules* **1987**, *20*, 1627.
(9) Salom, C.; Hernández-Fuentes, I.; Piérola, I. F.; Horta, A. *Macromolecules* **1989**, *22*, 1874.
(10) Maçanita, A. L.; Horta, A.; Piérola, I. F. *Macromolecules* **1991**, *24*, 1293.
(11) Salom, C.; Semlyen, J. A., Clarson, S.; Hernández-Fuentes, I.; Maçanita, A. L.; Horta, A.; Piérola, I. F. *Macromolecules* **1991**, *24*, 6827.
(12) Maçanita, A. L.; Danesh, P.; Peral, F.; Horta, A.; Piérola, I. F. *J. Phys. Chem.* **1994**, *98*, 6548.
(13) Maçanita, A. L.; Horta, A.; Piérola, I. F. *Macromolecules* **1994**, *27*, 958.
(14) Maçanita, A. L.; Horta, A.; Piérola, I. F. *Macromolecules* **1994**, *27*, 3797.
(15) Maçanita, A. L.; Horta, A.; Piérola, I. F. *Makromol. Chem., Macromol. Symp.* **1994**, *84*, 365.
(16) Wu, S. K.; Jiang, Y. C.; Rabek, J. F. *Polym. Bull.* **1980**, *3*, 319.
(17) Rubio, A.; Freire, J. J.; Piérola, I. F.; Horta, A. *Macromolecules* **1989**, *22*, 4014.
(18) Horta, A.; Piérola, I. F.; Rubio, A.; Freire, J. J. *Macromolecules* **1991**, *24*, 3121.
(19) Maçanita, A. L. *Plenary Lectures of the III Congreso de Fotoquímica*; UNED: Madrid, in press.
(20) Mark, J. E.; Ko, J. H. *J. Polym. Sci.: Polym. Phys. Ed.* **1975**, *13*, 2221.
(21) Freire, J. J.; Rubio, A. *J. Chem. Phys.* **1984**, *81*, 2112.
(22) Rubio, A.; Freire, J. J. *Macromolecules* **1985**, *18*, 2225.
(23) Mendicuti, F.; Tarazona, M. P.; Saiz, E. *Polym. Bull.* **1985**, *13*, 263.
(24) Llorente, M. A.; Piérola, I. F.; Saiz, E. *Macromolecules* **1985**, *18*, 2663.
(25) Salom, C.; Freire, J. J.; Hernández-Fuentes, I. *Polymer* **1989**, *30*, 615.
(26) Rubio, A.; Freire, J. J. *Macromolecules* **1989**, *22*, 333.
(27) Floudas, F.; Fytas, G.; Momper, B.; Saiz, E. *Macromolecules* **1990**, *23*, 498.
(28) Rubio, A.; Freire, J. J.; Horta, A.; Piérola, I. F. *Macromolecules* **1991**, *24*, 5167.
(29) Bahar, I.; Zúñiga, I.; Dodge, R.; Mattice, W. L. *Macromolecules* **1991**, *24*, 2986.
(30) Bahar, I.; Dodge, R.; Zúñiga, I.; Mattice, W. L. *Macromolecules* **1991**, *24*, 2993.
(31) Neuburger, N.; Bahar, I.; Mattice, W. L. *Macromolecules* **1992**, *25*, 2447.
(32) Bahar, I.; Neuburger, N.; Mattice, W. L. *Macromolecules* **1992**, *25*, 4619.
(33) Biosym Technologies, San Diego, CA.
(34) Grigoras, S. In *Computational Modeling of Polymers*; Bicerano, J., Ed.; Marcel Dekker: New York, 1992.

MA9517355